Joint Pathology Center
Veterinary Pathology Services

WEDNESDAY SLIDE CONFERENCE 2012-2013

Conference 24

8 May 2013

CASE I: 09-123996 (JPC 3170126).

Signalment: Three-month-old, female domestic shorthair cat (*Felis catus*).

History: The kitten came from a breeding colony at the College of Veterinary Medicine, Cornell University.

Gross Pathologic Findings: The kidneys are bilaterally enlarged; each measures approximately 4 x 3 x 2.5 cm. On section, the parenchyma exudes a small amount of clear fluid. Dozens of pinpoint to linear white foci are scattered throughout the cortex and medulla (tubular crystalluria).

Histopathologic Description: Kidney (1 section): Frequent tubules within the cortex and, to a lesser extent, the medulla, are occluded by linear crystalline material arranged into radiating sheaths. Crystals are translucent, clear to blue and birefringent bright white under polarized light (oxalate crystals). Cortical tubules are irregularly ectatic and variably lined by flattened, attenuated epithelium with hypereosinophilic cytoplasm and pyknotic nuclei (degeneration and necrosis) or, rarely, by plump, basophilic cells that are haphazardly stacked (regeneration). Scattered tubules additionally contain karyorrhectic debris and droplets of homogenous, eosinophilic material (protein). Small numbers of lymphocytes, plasma cells and neutrophils multifocally infiltrate the cortical and medullary interstitium and fine threads of fibroblasts occasionally dissect between tubules (fibrosis).

Contributor's Morphologic Diagnosis: 1. Kidney: Moderate, diffuse, subacute tubular necrosis and ectasia with multifocal tubular epithelial regeneration and many intratubular oxalate crystals.
2. Mild, multifocal lymphoplasmacytic and neutrophilic interstitial nephritis.

Contributor's Comment: This kitten was bred as a feline model of primary hyperoxaluria; the histologic features of the examined section of kidney are characteristic of this disease. Primary hyperoxaluria (PH) is best described in humans but has also been reported in cats, dogs and cattle.[2,3,4,5] In humans PH is a rare, autosomal recessive inherited disease that is classified as either type I (PH1) or type II (PH2) based on mutations of the respective genes alanine: glyoxylate aminotransferase (*AGT*) and glyoxylate

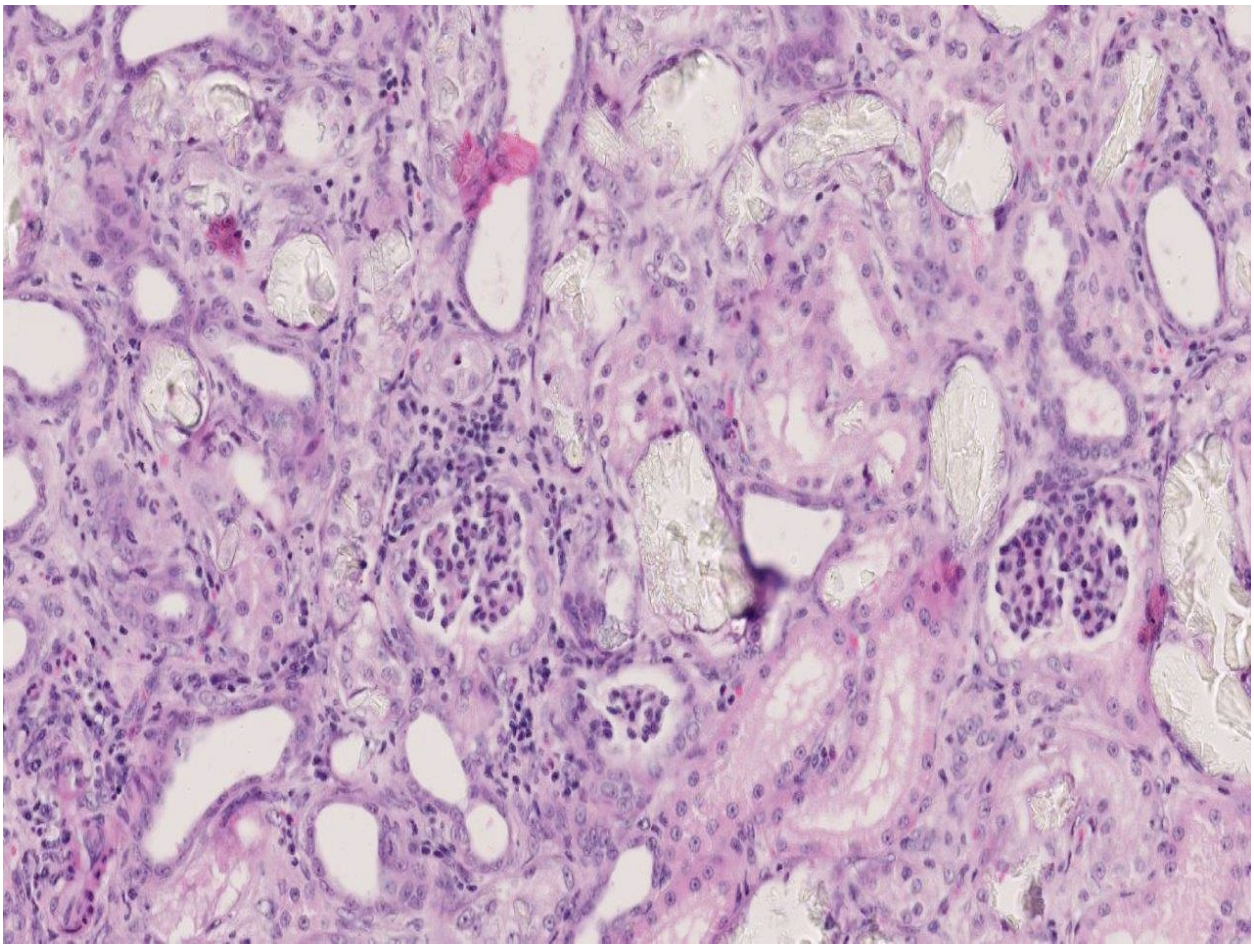

1-1. Kidney, cat: In this section of kidney from a 3-month-old kitten (note immature glomeruli) ectatic tubules contain numerous fan-shaped, birefringent oxalate crystals. Tubules are multifocally lined by attenuated epithelium and plump basophilic epithelium (regenerating epithelium). There is moderate interstitial fibrosis and lymphocytic interstitial inflammation. (HE 168X)

reductase/ hydroxypyruvate reductase (*GRHPR*), and their associated biochemical deficits. Up to 83 *AGT* mutations have been associated with PH1 and 13 mutations of *GRHPR* have been identified in cases of PH2; these mutations reduce or eliminate activity of the hepatic enzymes AGT and GRHPR.[1] Consequently, increased glyoxalate and hydroxypyruvate are available for conversion by lactate dehydrogenase to oxalate and, in the case of PH2, L-glyceric acid. The resultant errors in glyoxylate metabolism lead to markedly increased serum and urinary oxalate concentrations. Patients with PH2 also have L-glyceric aciduria as GRHPR mutations disrupt the hydroxypyruvate reductase pathway leading to production of L-glycerate in hepatocyte cytoplasm.[2,6] Mammals cannot metabolize oxalate, which is primarily excreted through the kidneys. In PH, oxalate binds with free calcium ions forming insoluble crystals; once the urine is super-saturated calcium oxalate crystals are deposited in renal tubules and, to a lesser extent, the renal interstitium. As renal excretion of oxalate declines, systemic deposition of calcium oxalate occurs and the retina, myocardium, central nervous system, skin, bone and blood vessel walls may be involved. Clinical disease in humans manifests by recurrent oxalate urolithiasis and nephrocalcinosis leading to end-stage renal failure and death, if untreated. Diagnosis is usually made when disease is already advanced; patients require dialysis and combined kidney and liver transplantation.[6]

A naturally occurring disease in cats, clinically similar to PH2 in humans, has been described in several instances.[2,3,4] As with humans, the disease is autosomal recessive and typically affects kittens between five and nine months of age. Affected animals develop acute renal

failure with increased urinary oxalate and L-glyceric acid levels. Histologically, abundant oxalate crystals are present within renal tubules and occasionally Bowman's spaces, accompanied by acute tubular necrosis and, variably, mild interstitial fibrosis.[3] Also consistent with human PH2, *GRHPR* mutation has been associated with the feline disease in cats from one colony.[4] A point mutation in the acceptor site of intron 4 was identified and correlated with a frameshift and premature stop codon in RNA transcripts from affected cats.

Several distinct differences exist in the clinical presentation of feline primary hyperoxaluria and PH2 in humans. Human PH2 is typically diagnosed in adults when renal changes are chronic; stone formation is usually less severe than that observed in PH1, which may present in infancy. By contrast, feline PH presents in young animals and is characterized by severe, acute disease. Concurrent neurologic lesions may accompany renal disease in cats and are histologically typified by swelling in the proximal axons of spinal motor neurons, ventral roots and intramuscular nerves and the dorsal root ganglia due to neurofilamentous accumulations. This lesion may be accompanied by Wallerian degeneration in peripheral nerves and associated denervation muscle atrophy. It is uncertain how these changes relate to the metabolic deficits present in primary hyperoxaluria or whether they represent a concurrent genetic defect.[3,7]

Primary hyperoxaluria must be distinguished from secondary disease due to exposure to large amounts of oxalates or increased absorption of dietary oxalic acid from the intestinal tract. In companion animals, acute oxalate nephrosis is typically seen in cases of ethylene glycol poisoning. In large animals, oxalate-rich plants are generally the source of toxicity.[8] Histologically, renal changes due to ethylene glycol toxicity are indiscernible from those present in cases of feline primary hyperoxaluria. A distinction between feline primary hyperoxaluria and oxalate toxicity is made on the basis of clinical history and supporting clinicopathological information (e.g. L-glyceric aciduria).

JPC Diagnosis: 1. Kidney: Tubular degeneration and necrosis, diffuse, marked, with regeneration, mineralization, and numerous intratubular oxalate crystals.
2. Kidney: Nephritis, interstitial, lymphoplasmacytic, multifocal to coalescing, mild, with fibrosis.

Conference Comment: The contributor provides an excellent synopsis of primary hyperoxaluria (PH). Given only the species of origin in advance of the conference, participants correctly determined that this was a young animal based on the occasional presence of hypercellular "fetal" glomeruli in the section. While most participants included PH in their differential diagnoses, ethylene glycol toxicosis was considered the most likely etiology. In addition to reviewing the pathogenesis of PH, conference participants discussed the pathogenesis of ethylene glycol toxicosis in depth. The main focus of the discussion was the clinicopathologic aberrations typical of ethylene glycol toxicosis, including titrational metabolic acidosis, hyperkalemia, hyperphosphatemia, hypocalcemia, and calcium oxalate monohydrate crystalluria.[9] A detailed review of ethylene glycol toxicosis and its associated clinicopathologic consequences is available elsewhere in these proceedings (i.e., Conference 18, Case III).

Finally, participants discussed toxic plants as the usual cause of oxalate nephrosis in ruminants. A partial listing of oxalate-containing plants implicated in such cases follows:[8]

Scientific Name	**Common Name**
Halogeton glomeratus	Halogeton
Sarcobatus vermiculatus	Greasewood
Rheum rhaponticum	Rhubarb
Oxalis cernua	Soursob
Rumex spp.	Sorrel, dock

Contributing Institution: Department of Anatomic Pathology
Biomedical Sciences
College of Veterinary Medicine
T4 018 Veterinary Research Tower
Cornell University

Ithaca, NY 14853
http://www.vet.cornell.edu/biosci/pathology/services.cfm

References:

1. Bobrowski AE, Langman CB. The primary hyperoxalurias. *Semin Nephrol*. 208;28:152-162.
2. Danpure CJ, Jennings PR, Mistry J, Chalmers RA, McKerrell RE, Blakemore WF, et al. Enzymological characterization of a feline analogue of primary hyperoxaluria type 2: a model for the human disease. *J Inherit Metab Dis*. 1989;12:403-14.
3. De Lorenzi D, Bernardini M, Pumarola M. Primary hyperoxaluria (L-glyceric aciduria) in a cat. *J Feline Med Surg*. 2005;7:357-361.
4. Goldstein RE, Narala S, Sabet N, Goldstein O, McDonough SP. Primary hyperoxaluria in cats is caused by a mutation in the feline GRHPR gene. *J Heredity*. 2009;100:S2-S7.
5. Gülbahar MY, Kaya A, Gölen I. Renal Oxalosis in a Calf. *Turk J Vet Anim Sci*. 2002;26:1197-1200.
6. Hoppe B, Beck BB, Miller DS. The primary hyperoxalurias. *Kidney Int*. 2009;75:1264-1271.
7. Maxie MG, Youssef S. Nervous system. In: Maxie MG, ed. *Jubb, Kennedy and Palmer's Pathology of Domestic Animals*. 5th ed. Philadelphia, PA: Elsevier Saunders; 2007:375.
8. Maxie MG, Newman SJ. Urinary system. In: Maxie MG, ed. *Jubb, Kennedy and Palmer's Pathology of Domestic Animals*. 5th ed. Philadelphia, PA: Elsevier Saunders; 2007:468-473.
9. George JW, Zabolotzky SM. Water, electrolytes, and acid base. In: Latimer KS, ed. *Duncan & Prasse's Veterinary Laboratory Medicine Clinical Pathology*. 5th ed. Ames, Iowa: Wiley-Blackwell; 2011:145-171, 430-432.

CASE II: 1984511 (JPC 4017822).

Signalment: 5-month-old male Boxer, dog (*Canis lupus familiaris*).

History: The puppy was presented with a two- to three-month history of waxing and waning occurrence of inappropriate mentation, visual difficulties and lethargy. The clinical neurologist concluded that the animal had multifocal disease of the thalamocortex and brainstem, which was thought somewhat worse on the right side. Due to a poor prognosis, the puppy was euthanized. The brain was removed and portions submitted for rabies testing, which was negative, prior to postmortem examination of the rest of the body.

Gross Pathology: The puppy weighed 10.5 kg, had adequate fat stores, and, at the time of somatic necropsy after rabies testing, was severely autolyzed. No other gross findings were noted.

Laboratory Results: Negative rabies IFA at the public health department laboratory.

Histopathologic Description: Brain: The gray matter and immediately adjacent white matter of the medulla, excluding the vagal and hypoglossal nuclei, contain numerous lacey, irregularly interconnected, unstained vacuoles that are well defined. At the edges of some affected areas astrocytes possess enlarged, pale homogeneous nuclei. The gray matter of the caudate nucleus, globus pallidus, peri-aqueductal gray matter, parts of the reticular formation, thalamus and hypothalamus are similarly affected, with much less change in the cerebrum and cerebellum.

Liver: The hepatic lobules are mildly reduced in size. Although thin-walled veins are present in the largest portal areas near the capsule of the liver, none are apparent in the portal triads comprising the liver parenchyma.

Contributor's Morphologic Diagnosis: 1. Brain: Spongiform encephalopathy, gray matter, with astrocytic nuclear hypertrophy (Alzheimer type II astrocytes).
2. Portal vein hypoplasia, liver.

Contributor's Comment: Hepatoencephalopathy occurs in the presence of liver injury or, as in this case, if the liver is bypassed due to a portosystemic shunt.[1] Prominent histopathological changes found in encephalopathy that accompanies liver failure include Alzheimer's type II astrocytosis (i.e. enlarged astrocytes with pale, large nuclei and prominent nucleoli) and pronounced astrocytic swelling, leading to spongiform change. Hepatoencephalopathy can result from acute or chronic liver failure, including that resulting from portocaval shunts, and is considered to result from accumulation of toxic substances, principally ammonia, but impaired

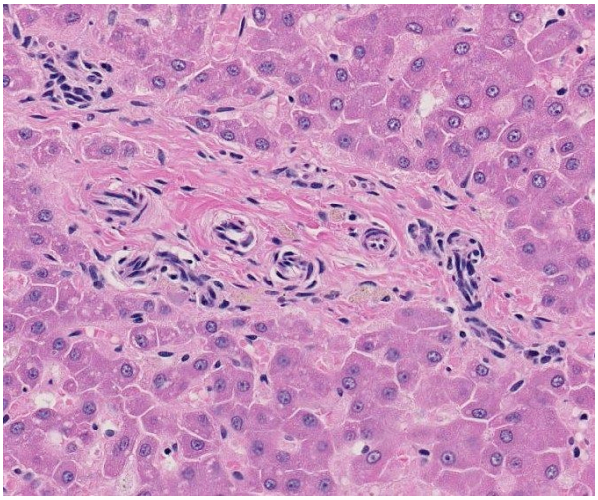

2-1. Liver, 5-month-old Boxer: Portal areas contain numerous cross sections of hepatic arterioles, without a single portal vein. Surrounding hepatocytes are decreased in size (atrophy). These changes are characteristic of microvascular dysplasia. (HE 220X)

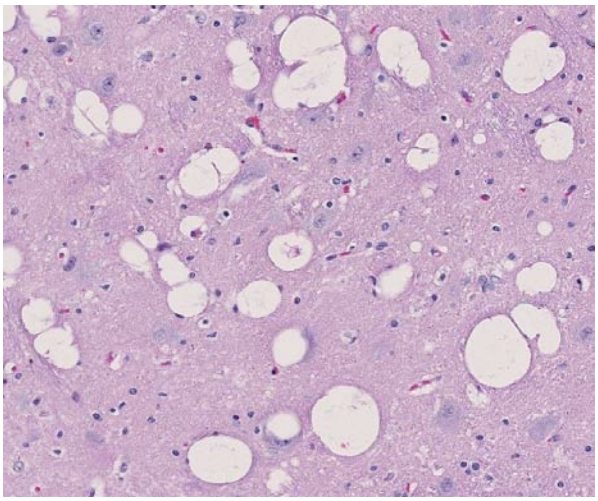

2-2. Cerebrum, 5-month-old Boxer: The grey matter contains numerous clear discrete vacuoles (spongiosis). (HE 100X)

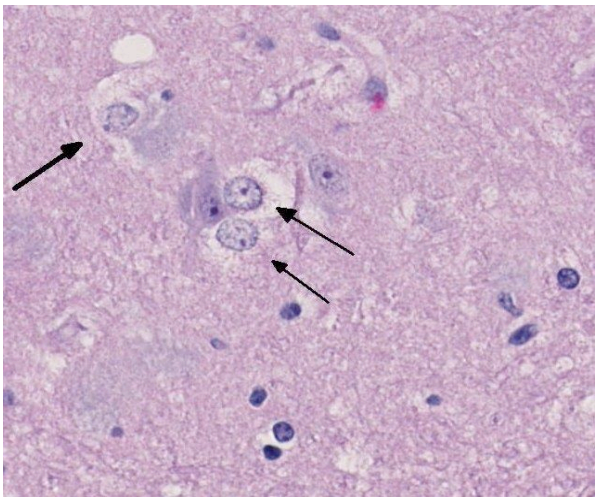

2-3. Cerebrum, 5-month-old Boxer: Within the spongiotic section of the cerebrum, there are moderate numbers of astrocytes with moderate amounts of amphophilic cytoplasm and large, vesicular nuclei (Alzheimer's Type II astrocytes). (HE 140X)

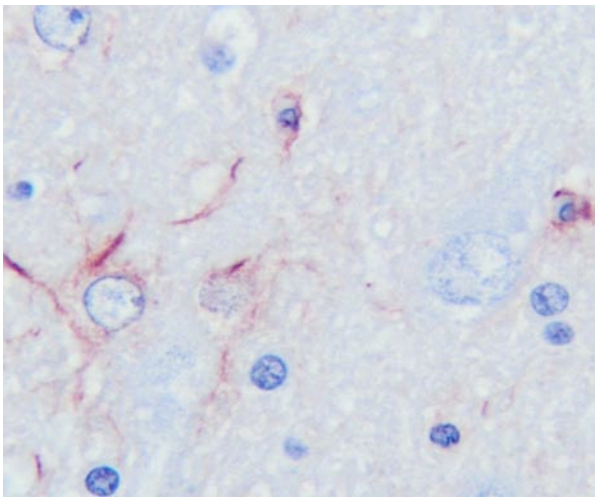

2-4. Cerebrum, 5-month-old Boxer: Alzheimer's Type II astrocytes exhibit poor staining with glial fibrillary acidic protein> (HE 280X). (Photo courtesy of: The Veterinary Medical Diagnostic Laboratory and Department of Veterinary Pathobiology, University of Missouri, http://www.cvm.missouri.edu/vpbio)

detoxification during liver failure results in increased blood levels of several toxic compounds.

In acute liver failure, spongiform encephalopathy may lead to increased intracranial pressure. Studies suggest that intracranial hypertension complicates 25% of acute liver failure cases in humans but only 9% of those with subacute liver failure. In acute liver failure, an arterial ammonia concentration greater than 150 µmol/L predicts a greater likelihood of dying from brain herniation.[1] Spongiform change can be found in a variety of species, with the exception of the horse.

Of the compounds that escape detoxification by the failing liver, ammonia most easily crosses the blood-brain barrier. Although other compounds contribute, ammonia is accepted as the central cause of hepatoencephalopathy. It is considered that astrocyte dysfunction is central to ammonia toxicity in hepatoencephalopathy, and that functional neuronal changes are secondary. Astrocytic end processes surround capillaries in the CNS. Normally, this would ensure that any toxin entering the brain, such as ammonia, would be immediately metabolized, protecting other CNS cells from damage. In acute liver failure, increased brain ammonia concentrations affect transit of electrolytes and water across cell membranes, and cause astrocyte swelling, with cytotoxic brain edema. Primary alteration of the blood brain barrier results in vasogenic edema as well. Opening of the blood-brain barrier is thought to further exacerbate aberrant neuronal transmission and entry of toxins besides ammonia. Immunohistochemical staining with GFAP demonstrates some astrocytes with dense robust processes, while others near vacuoles stain poorly. CD18 reagent revealed multifocal clusters of large cells, with microglial morphology in affected tissue.

Astrocytes perform a number of other important metabolic supportive functions for neurons, including supplying them with GSH, the main cytosolic antioxidant.[2] Significant reduction in the activities of glutathione peroxidase and superoxide dismutase enzymes occur in the brain of rats exposed to ammonium acetate.[1]

Astrocytes also control GABAergic and glutamatergic activities at the synapse, especially terminating excitotoxic action in the synaptic cleft. Astrocytes take up glutamate, metabolizing it to glutamine that is transported back to excitatory neurons for neurotransmitter metabolism. In hepatoencephalopathy, there is correlation between astrocyte swelling and glutamine concentration. When the urea cycle is dysfunctional in the brain, ammonia is detoxified through its condensation with glutamate to form glutamine. Increased ammonia concentrations lead to mitochondrial permeability transition, and the loss of

mitochondrial transmembrane potential.[1] Astrocytes also utilize glycolysis to produce lactate as a neuronal energy source.

There are additional roles for inflammation in hepatoencephalopathy. In advanced stages of acute liver failure, the brain produces a number of pro-inflammatory cytokines such as tumor necrosis factor-α (TNF-α), interleukin (IL)-1β and IL-6.

JPC Diagnosis: 1. Liver: Venous hypoplasia, portal and central, diffuse, marked, with arteriolar hyperplasia, lymphangiectasia, and mild lobular and hepatocellular atrophy.
2. Cerebral cortex, gray matter: Spongiform change, multifocal to coalescing, marked, with Alzheimer type II astrocytosis and microgliosis.

Conference Comment: Conference participants readily ascribed the lesions in the cerebral cortex to hepatoencephalopathy, and recognized the salient diagnostic features of a portosystemic shunt (PSS) in the liver. Attendees briefly reviewed canine congenital PSS, which are usually caused by a single large anomalous connection between the portal venous and systemic venous circulation. Intrahepatic shunts are most common in large-breed dogs and usually consist of a patent fetal ductus venosus in the left hepatic division. Extrahepatic shunts, more common in small-breed dogs and cats, usually consist of a direct shunt from the portal vein, gastric vein, or splenic vein to the caudal vena cava (i.e., portocaval shunt), or to the azygous vein (i.e., portoazygous shunt). Importantly, congenital PSS do not result in portal hypertension, whereas other congenital vascular anomalies, such as congenital arteriovenous fistulae, primary hypoplasia of the portal vein, and hepatoportal microvascular dysplasia, do cause portal hypertension, and can thus lead to ascites and the development of acquired portosystemic shunts.[3]

The conference moderator led a review of the serum biochemistry abnormalities typical of PSS with hepatic atrophy. Fasting and postprandial serum bile acid concentrations are elevated for at least two reasons: 1) portal blood has a high concentration of bile acids, and bypasses the liver, which in health removes approximately 95% of bile acids from portal blood; and 2) hepatic atrophy that follows chronic shunting causes loss of hepatic functional mass, impairing the liver's ability to clear bile acids from the blood. Hyperammonemia, as discussed by the contributor, is also usually present in PSS because ammonia bypasses the liver, where hepatic urea cycle enzymes catalyze its conversion to urea. Consequently, animals with PSS may develop ammonium biurate crystalluria, as ammonium biurate precipitates in alkaline urine. With chronicity and the development of hepatic atrophy, loss of hepatic functional mass may result in hypoalbuminemia, hypoglycemia, hypocholesterolemia and/or decreased blood urea nitrogen (BUN) concentrations. Levels of cholestatic markers (e.g. alkaline phosphatase, gamma glutamyltransferase) and hepatocellular leakage enzymes (e.g. alanine transaminase, aspartate transaminase, sorbitol dehydrogenase, glutamate dehydrogenase) are usually within reference intervals. Animals with PSS may have microcytic anemia of unknown cause.[4]

Contributing Institution: Veterinary Medical Diagnostic Laboratory and Department of Veterinary Pathobiology
University of Missouri
http://www.cvm.missouri.edu/vpbio

References:

1. Seyan AS, Hughes RD, Shawcross DL. Changing face of hepatic encephalopathy: role of inflammation and oxidative stress. *World J Gastroenterol.* 2010;16:3347-3357.
2. Sidoryk-Wegrzynowicz M, Wegrzynowicz M, Lee E. Bowman AB, Aschner M. Role of astrocytes in brain function and disease. *Toxicol Pathol.* 2011;13:115-123.
3. Stalker MJ, Hayes MA. Liver and biliary system. In: Maxie MG, ed. *Jubb, Kennedy and Palmer's Pathology of Domestic Animals*. 5th ed. Philadelphia, PA: Elsevier Saunders; 2007:2:302-304.
4. Bain PJ. Liver. In: Latimer KS, ed. *Duncan & Prasse's Veterinary Laboratory Medicine Clinical Pathology*. 5th ed. Ames, Iowa: Wiley-Blackwell; 2011:227, 415-417.

CASE III: S1269/08 (JPC 3138060).

Signalment: 17-year-old gelded Westfalian warmblood, horse (*Equus caballus*).

History: The horse had an eight-week history of pneumonia. Physical examination revealed a reduced nutritional status, and a purulent exudate was detected within the trachea. Microbiological investigation yielded growth of *Aspergillus fumigatus* within the tracheal fluid. Based on the thoracic radiography results, a granulomatous pneumonia was suspected. Due to unsuccessful treatment, the horse was eventually euthanized for animal welfare reasons.

Gross Pathologic Findings: The horse was in a reduced nutritional condition. Necropsy revealed that the main lesions were restricted to the lung. Lung parenchyma was interspersed with multiple large, bulging, coalescent, tan to white and firm nodules of fibrosis affecting all lobes. The patchy areas of fibrosis had predominantly distinct borders to the adjacent normal appearing lung tissue. The cut surfaces of the nodules were homogeneously tan to white. Numerous subpleural hyperemic blood vessels and emphysema of the cranial lung lobes were additionally detected. The bronchial lymph nodes were noticeably enlarged. Furthermore, the trachea revealed a streaky redness of mucosa.

Laboratory Results: Lung: DNA of both equine herpesvirus type 5 (EHV-5) and EHV-2 was detected using standard PCR analysis.
Tracheal fluid: mild growth of *Candida* species.

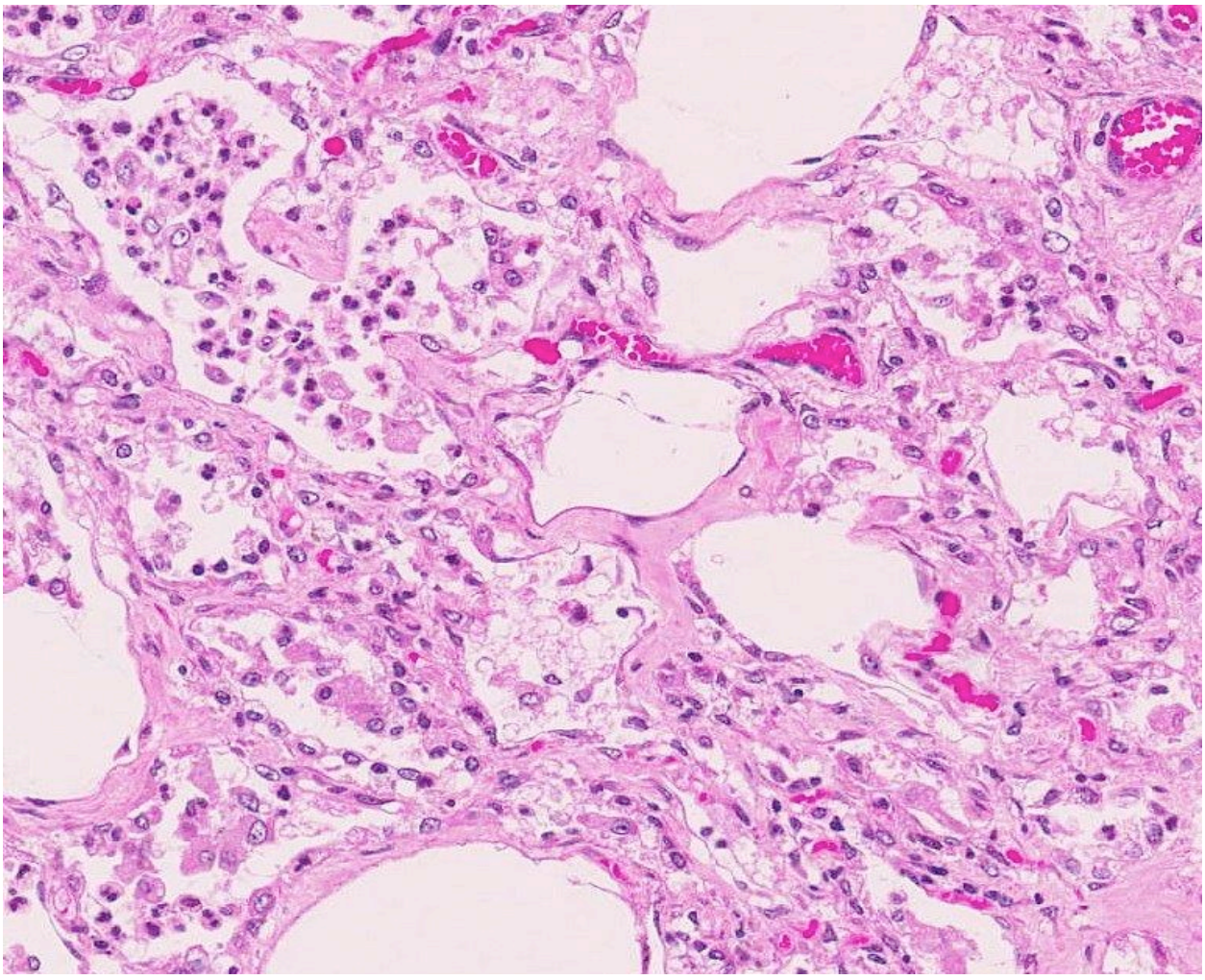

3-1. Lung, horse: Diffusely throughout the section, alveolar septa are thickened up to ten times by a combination of mature collagen (center), plump fibroblasts, and type II pneumocytes hyperplasia. Alveolar spaces contain moderate numbers of neutrophils and macrophages. (HE 256X)

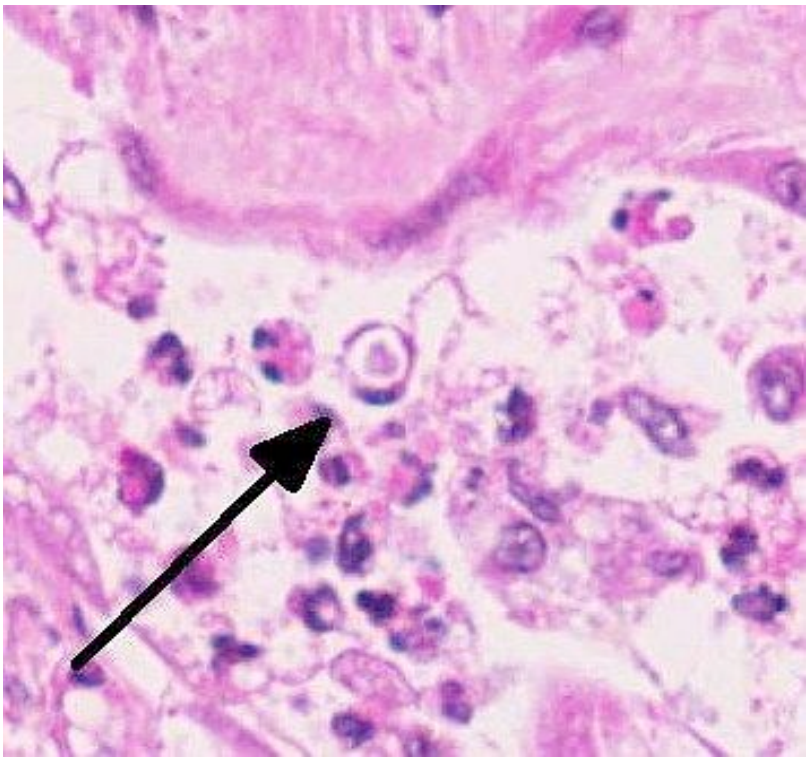

3-2. Lung, horse: Within alveolar spaces, macrophage nuclei occasionally contain a single 4µm eosinophilic viral inclusion surrounded by a clear halo. (HE 400X)

Histopathologic Description: The lung fibrosis resulted in a vast interstitial expansion and eventually led to a complete remodeling of the lung architecture and formation of abnormal cystic airspaces (honeycombing). These airspaces were lined by a cuboidal epithelium. According to the gross findings, the nodular lesions were sharply demarcated from normal parenchyma. The interstitium was infiltrated by numerous inflammatory cells including lymphocytes, plasma cells and neutrophils as well as some eosinophils and multinucleated giant cells. The bronchioli, alveoli, and abnormal cystic airspaces were filled with numerous large vacuolated macrophages and neutrophils. Occasionally, some multinucleated giant cells were detected. Within lung areas with chronic inflammatory lesions, a few enlarged intraluminal macrophages were found that showed eosinophilic intranuclear inclusion bodies (Cowdry type A). Some lung areas revealed a marked alveolar edema and hyperplasia of type II pneumocytes. Special stains for bacteria and fungi yielded negative results. The bronchiolar lymph nodes were severely hyperplastic. Acute hemorrhages were found within submucosal and muscular layers of the trachea. No inflammation and no pathogenic agents were detectable within the tracheal mucosa using special staining methods.

Contributor's Morphologic Diagnosis: Lung: Equine multinodular pulmonary fibrosis (EMPF).

Contributor's Comment: Equine multinodular pulmonary fibrosis (EMPF) is a chronic and fibrosing interstitial lung disease in adult horses that results in characteristic lung lesions. The disease was first recognized in 2005 by Williams et al.[1] and further cases in the USA and Europe have recently been described.[2-5] In all reported cases, the disease was associated with an infection of EHV-5, which belongs to the genus percavirus that is actually classified within the gammaherpesvirus subfamily.[6] A co-infection with EHV-2 was detected in several cases, but it seems not to be associated with EMPF.[2,3,5] In horses suffering from EMPF, the lung lesions differ significantly from other interstitial fibrosis in lung diseases due to their nodular pattern, the parenchymal remodeling with honeycombing and the presence of intranuclear viral inclusion bodies within intraluminal macrophages. Other noxa, such as thermal and chemical injury, toxic gases, ingested toxins, endotoxins, pneumoconiosis, uremia and chronic left heart failure could be excluded in the present case as cause for interstitial pneumonia. The pathogenesis of EMPF is unclear at the moment.

JPC Diagnosis: Lung: Fibrosis, interstitial, diffuse, severe, with histiocytic and neutrophilic alveolitis, type II pneumocyte hyperplasia and rare eosinophilic intrahistiocytic intranuclear viral inclusions.

Conference Comment: As noted by the contributor, Koch's postulates have not yet been fulfilled to definitively establish EHV-5 as the

etiology of EMPF. Moreover, asinine herpesvirus-5 (AHV-5) has also been detected by PCR either alone, or in combination with EHV-5, in some cases of EMPF, suggesting that other herpesviruses may be involved in the pathogenesis of the disease. An analogous human condition, idiopathic pulmonary fibrosis (IPF) is similarly attributed to an array of potential causes, including pneumocyte injury, abnormal fibroplasia, inflammation, and the excessive deposition of extracellular matrix proteins. As with EMPF, gammaherpesviruses have been implicated in the pathogenesis and/or exacerbation of IPF, as well as IPF-like lesions in mice.[7]

Conference participants discussed the importance of the cytokine milieu in driving macrophage activation and expression, and speculated that, based on the degree of fibroplasia that typifies EMPF, alternative (M2) activation of macrophages is most likely to predominate in this condition. Monocytes exposed to the signature cytokines of Th2 lymphocytes (i.e., IL-4 and IL-13) undergo alternative (M2) activation to mature into a fibrotic phenotype and produce polyamines that drive cell proliferation, and proline and TGF-β that drive collagen production.[8]

Other notable gammaherpesviruses of importance in animals were briefly reviewed, including those associated with IPF-like lesions in the lungs of mice (i.e., Murine herpesvirus-68), urogenital carcinomas in California sea lions (i.e., Otarine herpesvirus-1), and malignant catarrhal fever in ruminants (i.e., Alcelaphine herpesvirus-1, Alcelaphine herpesvirus-2, Hippotragine herpesvirus-1, Ovine herpesvirus-2, Caprine herpesvirus-2 and MCFV-white tailed deer).

Contributing Institution: Institute of Veterinary Pathology
Ludwig-Maximilians-University Munich
Veterinaestrasse 13
D-80539
Munich Germany
www.patho.vetmed.uni-muenchen.de

References:

1. Williams KJ, Jackson CA, Scott MA, Robinson NE, Derksen FJ, Macs R, et al. Multinodular equine pulmonary fibrosis: a newly recognized herposvinis associated respiratory disease of horses. ACVP/ASVCP meeting. *Vet Pattie'*. 2005;42:716.
2. Williams KJ, Maes R, Del Piero F, Lim A, Wise A, Bolin DC, et al. Equine multinodular pulmonary fibrosis: a newly recognized herpesvirus-associated tihtotic lung disease. *Vet Pathol*. 2007;44:849-862.
3. Hart KA, Barton MH, Williams KJ, Flaminio MJBF, Howerth EW. Pulmonary fibrosis, pancytopenia and equine herpesvirus-5 infection in a Thoroughbred gelding. *Equine Vet Educ*. 2008;20:470-6.
4. Wong DM, Belgrave RL, Williams KJ, Del Piero F, Alcott CJ, Bolin SR, et al. Multinodular pulmonary fibrosis in five horses. *J Am Vet Med Assoc*. 2008;232:898-905.
5. Poth T, Niedermaier G, Hermanns W. Equine multinodular pulmonary fibrosis (EMPF) in association with an EHV-5 infection in 5 horses. *Wien Tierailtl Monatsschr.* 2009;96:203-8.
6. McGeoch DJ, Rixon FJ, Davison AJ. Topics in herpesvirus genomics and evolution. *Virus Res*. 2006;117:90-104.
7. Back H, Kendall A, Grandon R, Ullman K, Treiberg-Berndsson L, Stahl K, et al. Equine multinodular pulmonary fibrosis in association with Asinine herpesvirus type 5 and Equine herpesvirus type 5: a case report. *Acta Veterinaria Scandinavica*. 2012;54:57.
8. Ackermann MR. Inflammation and healing. In: Zachary JF, McGavin MD, eds. *Pathologic Basis of Veterinary Disease*. 5th ed. St. Louis, MO: Elsevier; 2012: 128-130.

CASE IV: 10L-3893 (JPC 4002755).

Signalment: 18-month-old, female, Cavalier King Charles Spaniel, dog (*Canis familiaris*).

History: 48-hour history of hematochezia, icterus and collapse with marked anemia (PCV 7%) with regeneration. Prior to presentation the referring veterinary surgeon removed a gastric metallic foreign body, an identification tag, via gastrotomy.

Gross Pathology: There was moderate to severe icterus observed throughout the subcutis, sclera and visceral adipose tissue. The cut surfaces of both kidneys were diffusely very dark red. The urinary bladder contained a small volume of red-tinged urine (pigmenturia). The pancreas was diffusely pale and nodular, and on the cut surface there were multifocal, variably sized (~2 mm – 1 cm), dark red, approximately spherical to irregularly shaped, soft foci (necrosis). The descending colon and rectum contained a moderate amount of soft, red-tinged fecal material (evidence of hematochezia).

Laboratory Results:

Haematology - PCV 7%
- degenerative left shift
- reticulocytes 5%

Biochemistry - urea 45.7 mmol/l (3.5 – 6.0)
- creatinine 243 µmol/l (20 – 110)
- ALP 497 U/l (0 – 100)
- ALT 136 U/l (7 – 50)

APTT -123 seconds (8 -12)

Tissue chemical analysis

Test	Units (Wet weight)	Ref range (normal)	Ref (toxic)	CASE
Zinc (Liver)	ppm	30-70	204-436	165
Zinc (Kidney)	ppm	16-30	190-295	141

Histopathologic Description: Kidney: Multifocally within renal tubular lumina throughout the cortex and medulla, there is moderate to marked accumulation of eosinophilic material which varies from coarsely granular to hyaline or crystalloid (hemoglobin). Similar coarsely granular, eosinophilic material is also present within vascular lumina, and no intact erythrocytes are observed. Multifocally, tubular epithelial cells are expanded by mild to moderate accumulation of cytoplasmic eosinophilic material (hemoglobin). There are focal areas where tubular epithelial cells appear hypereosinophilic with nuclei exhibiting clumped chromatin or karyorrhexis (acute tubular necrosis). There are mild, multifocal infiltrates of lymphocytes (mild, tubulo-interstitial nephritis). There is focally mild accumulation of coarsely granular eosinophilic material within the urinary space of glomeruli.

Pancreas: Throughout the exocrine pancreas there are multifocal, variably sized (2-5 mm), irregularly shaped, moderately well demarcated areas characterized by hypereosinophilia of the acinar cells and disruption of acinar architecture (necrosis). The centers of these foci exhibit disorganized accumulations of proteinaceous and nuclear debris with some nuclei exhibiting pyknosis and karyorrhexis, with few scattered acinar cells remaining. Multifocally at the periphery of these foci and within sub-capsular connective tissue are variable numbers of neutrophils. Pancreatic lobules are separated by mildly edematous interstitium. Peripancreatic and interstitial adipose tissue often contains foci of amorphous basophilic to amphophilic material with numerous macrophages with vacuolated cytoplasm (foamy) with neutrophils and spindloid cells with plump, ovoid nuclei (fat necrosis).

Some sections also contain a small amount of unaltered duodenum.

Contributor's Morphologic Diagnosis: 1. Kidney – multifocal to diffuse, moderate intratubular and intravascular hemoglobin accumulation with hemoglobin cast formation, with mild, multifocal acute tubulonecrosis and mild, multifocal, chronic, lymphocytic tubulo-interstitial nephritis.

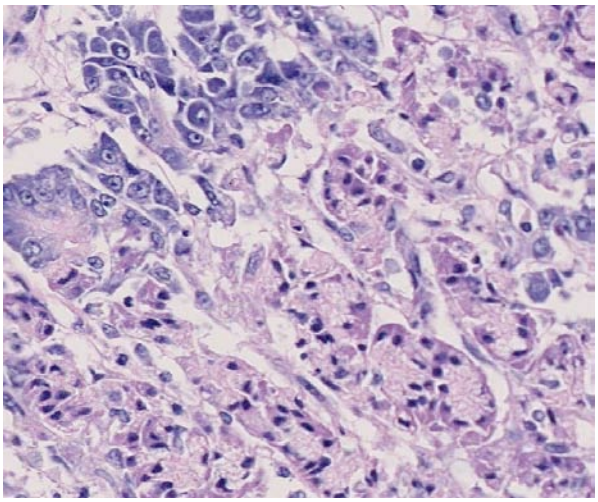

4-1. Pancreas, dog: There is extensive necrosis of pancreatic acinar tissue. Adjacent viable pancreatic acini show degenerative changes, including disorganization of acinar architecture and loss of zymogen granules. (HE 284X)

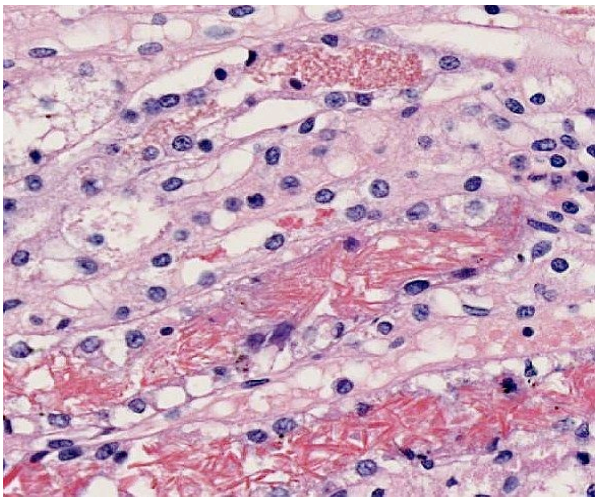

4-2. Kidney, dog: Throughout the kidney (here in the medulla), tubular lumina are filled with a bright red granular material (hemoglobin) which forms granular (top), and specular arrangements. (HE 284X)

2. Pancreas – multifocal, severe, acute pancreatic necrosis with mild acute neutrophilic pancreatitis and fat necrosis.

Contributor's Comment: The pathological changes confirmed the clinical suspicion of acute hemolytic anemia by demonstrating marked intratubular and intravascular accumulation of hemoglobin; the hyaline hemoglobin casts being a typical presentation. Staining of sections of kidney with Dunn-Thompson's stain confirmed the hyaline tubular casts to be hemoglobin. There were also areas of mild acute tubulonecrosis and inflammation. Acute pancreatic necrosis was also demonstrated. These findings, together with the history of prior removal of a metallic gastric foreign body, lead to the presumptive diagnosis of zinc intoxication, which was confirmed by the markedly raised levels of zinc in the liver and kidney. Although the zinc levels in liver and kidney post-mortem are below the reference toxic range, it has been shown in similar cases that after removal of the offending foreign body, zinc levels decline rapidly, and it is considered likely that in this case tissue levels would have been higher whilst the foreign body was present in the stomach.[11]

Zinc intoxication has been reported in the USA on several occasions since the mid 1980s, often as a consequence of ingestion of zinc-containing coins;[4] there have also been cases reported in Europe.[1,2] In a review of 19 cases, the most common presenting clinical signs included hemolytic anemia, gastrointestinal disturbances and pigmenturia.[4] Acute pancreatic necrosis (acute pancreatitis) has been reported previously in only two dogs.[8,11] Zinc toxicity may result from ingestion of zinc-containing metallic foreign bodies as the acidic pH of gastric secretions liberates zinc which facilitates absorption, it is bound to albumin and macroglobulins where it is transported to the liver before being distributed to pancreas, kidney and spleen.[3]

The mechanism underlying the zinc-associated hemolysis is not completely elucidated. Suggested mechanisms include oxidative injury due to inhibition of glutathione reductase or enzymes of the hexose-monophosphate pathway,[5] however, oxidative stress often leads to Heinz body formation in erythrocytes, and in the aforementioned review, only 33% of cases exhibited Heinz body formation, suggesting other mechanisms may also be present.[4] During clinical examination, biochemical analysis revealed azotaemia in this case, and histological examination of the kidneys revealed scattered areas of acute tubulonecrosis. Zinc is not considered to be a direct nephrotoxin, but the marked hemolysis and intratubular accumulation of hemoglobin is likely to have lead to hemoglobinuric nephrosis. In this condition, while hemoglobin is not a primary nephrotoxin it is thought to lead to an ischemic necrosis through other

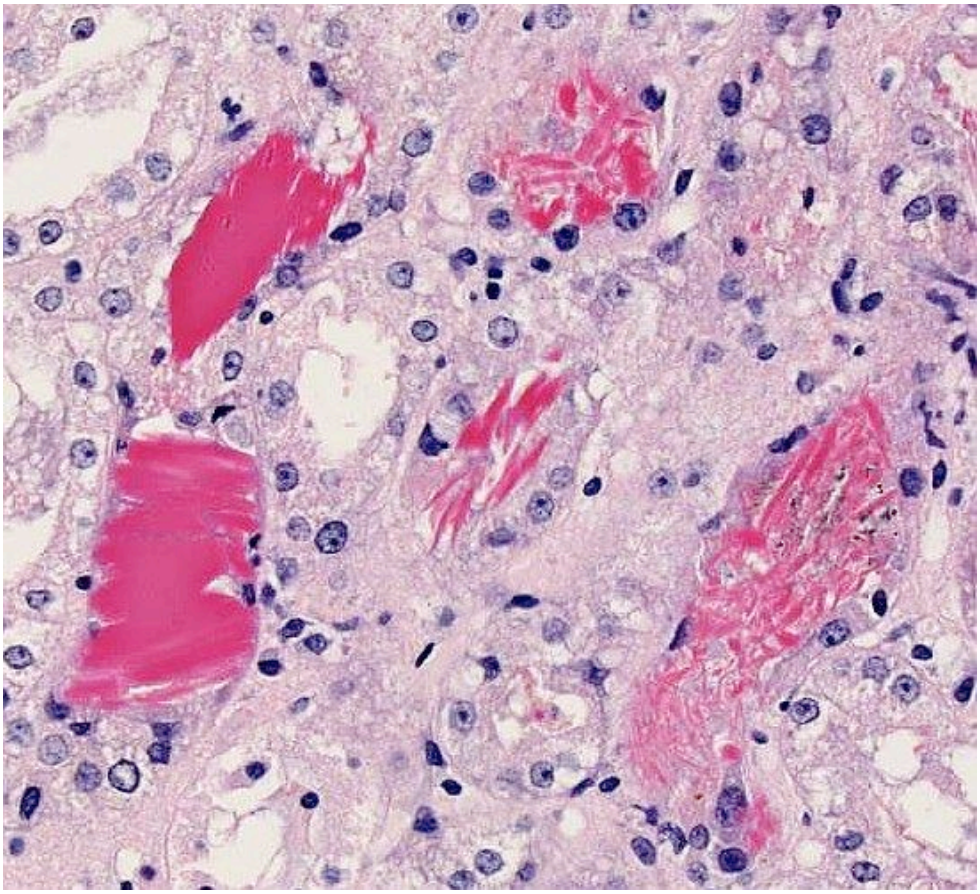

4-3. Kidney, dog: Within he proximal convoluted tubules, sheave-like arrangements of crystalling hemoglobin aggregate to form large bright red sheets. (HE 310X)

mechanisms such as hypotension.[6] The extended activated partial thromboplastin time is of uncertain pathogenesis, but it has been hypothesized that zinc may inhibit certain coagulation factors, e.g. VIII, IX, XI and XII.[7]

The mechanism underlying the acute pancreatic necrosis is similarly poorly defined. Zinc has been shown to be concentrated in the pancreas of the dog,[8] and to cause acute acinar cell necrosis and pancreatitis in mice.[9] The pancreas plays an important part in zinc homeostasis and contains high levels of metallothionein (MT). In studies on zinc-induced pancreatitis in mice, pretreatment with non-toxic doses of zinc protect the pancreas from a toxic dose if given 24 hours prior to the toxic dose, apparently by induction of MT which is able to sequester excess zinc.[9,10] If the pretreatment is given 2 hours prior to the toxic dose or no pretreatment is given, however, the toxic mechanism in mice appears to be related to free zinc ions or zinc bound to low molecular weight proteins, and there is no increase in the MT-bound fraction.[10] These studies also showed that pre-treatment of the mice with a trypsin inhibitor before zinc challenge attenuated the signs of pancreatitis, i.e. serum amylase activity, suggesting that zinc-induced pancreatitis may be related to activation of trypsinogen. The underlying mechanism remains unclear, although there has been speculation over the role of oxidative stress in the pancreas.[10]

JPC Diagnosis: 1. Pancreas: Acinar degeneration and necrosis, acute, multifocal to coalescing, marked with edema, necrosis and saponification of peripancreatic adipose tissue.
2. Kidney, tubules: Degeneration and necrosis, acute, diffuse, marked, with tubulorrhexis, edema and many intratubular protein and hemoglobin casts.

Conference Comment: The contributor provides an excellent review of zinc toxicosis. The submitted section of kidney provides for an edifying contrast with Case I from this conference. While both sections feature abundant tubular degeneration and necrosis, a key difference is the presence of tubulorrhexis in this case. Tubulorrhexis, or necrosis of the tubular epithelial cells accompanied by rupture or loss of the basement membrane, is often a consequence of ischemic damage. Its presence in this case supports the idea, noted by the contributor, that ischemia is at least part of the

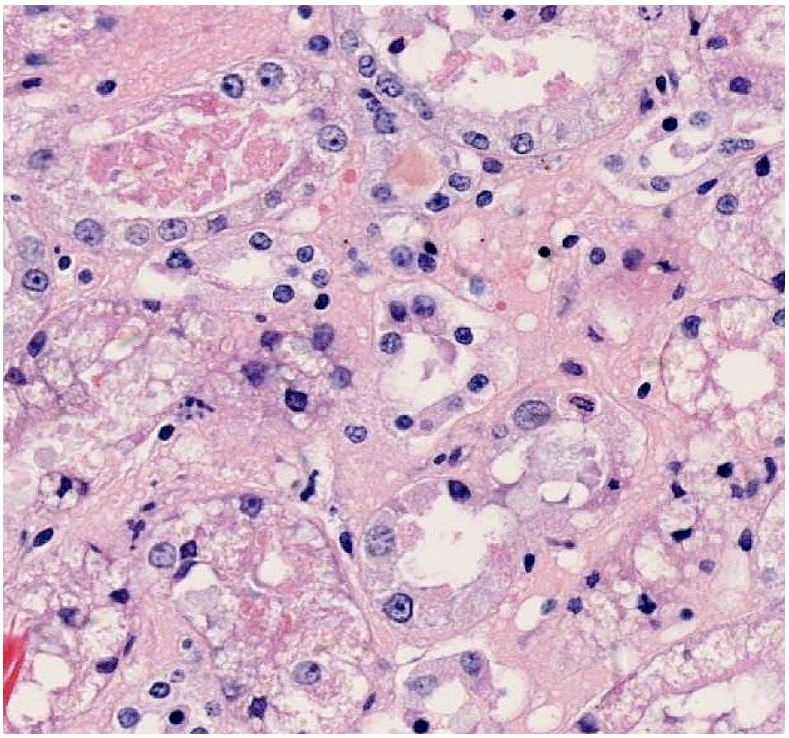

4-4. Kidney, dog: Throughout the cortex, the epithelium of proximal convoluted tubules is degenerate or necrotic (acute tubular necrosis). There is extensive interstitial edema, and many tubules contain hemoglobin wither within the cytoplasm of epithelial cells, or within the lumen. (HE 310X)

mechanism underlying hemoglobinuric nephrosis. In addition to providing clues to the mechanism of tubular damage, the presence of tubulorrhexis has important implications for the ability of the tubule to respond to injury. Although glomeruli are essentially incapable of regeneration, tubular epithelial cells can regenerate and reepithelialize the tubule following injury as long as the basement membrane remains intact, as was evidenced in case 1. Intact basement membranes not only form an effective barrier system for defense against injury and infectious agents; they also form the scaffolding for tubule reepithelialization.[12]

Zinc toxicosis uniformly topped conference participants' differential diagnoses based on the combination of pancreatic and renal lesions evident in this case. Other common causes of hemoglobinuric nephrosis include immune-mediated hemolytic anemia in dogs, red maple leaf toxicosis in horses, babesiosis in dogs and cattle, leptospirosis in cattle, and chronic copper toxicosis in sheep.[12] In intravascular hemolysis, free hemoglobin is bound by an α2-globulin carrier, haptoglobin; hemoglobin-haptoglobin complexes are cleared by the liver, preventing loss of hemoglobin in the urine. Haptoglobin is usually present in sufficient quantities to bind hemoglobin up to 150 mg/dL. Since hemoglobin causes pink to red discoloration of plasma at much lower concentrations (i.e. 50-100 mg/dL), plasma discoloration precedes the development of hemoglobinuria. When haptoglobin becomes saturated, excess hemoglobin dissociates into dimers, which pass freely through the glomerulus, and are absorbed by the proximal convoluted tubule and catabolized to iron, bilirubin, and globin. Excess unabsorbed hemoglobin passes into the urine, causing hemoglobinuria.[13]

Conference participants briefly reviewed the differential diagnosis for causes of red-brown urine with a positive occult blood test: hematuria, hemoglobinuria, and myoglobinuria. Hematuria usually clears with centrifugation; the presence of erythrocytes in the urine sediment and absence of clinical or laboratory evidence of hemolytic anemia or muscle disease are also supportive of the diagnosis. Neither hemoglobin nor myoglobin will clear upon centrifugation of urine; however, the addition of saturated ammonium sulfate solution will clear the urine sample by precipitating hemoglobin. Clinical evidence of intravascular hemolysis and the presence of pink to red discolored plasma further support the diagnosis. Saturated ammonium sulfate will not clear myoglobin from the urine, and the plasma should remain clear.[14]

Contributing Institution: School of Veterinary Science
University of Liverpool
Crown Street
Liverpool
L69 7ZJ
United Kingdom
www.liv.ac.uk/vets/index.htm

References:

1. Bexfield N, Archer J, Herrtage M. Heinz body haemolytic anaemia in a dog secondary to ingestion of a zinc toy: a case report. *Vet J*. 2007;174:414-417.
2. Gandini G, Bettini G, Pietra M, Mandrioli L, Carpene E. Clinical and pathological findings of acute zinc intoxication in a puppy. *J Small Anim Pract*. 2002;43:539-542.
3. Garland T. Zinc. *Veterinary Toxicology - Basic and Clinical Principles*. Oxford, UK: Elsevier; 2007.
4. Gurnee CM, Drobatz KJ. Zinc intoxication in dogs: 19 cases (1991-2003). *J Am Vet Med Assoc*. 2007;230:1174-1179.
5. Luttgen PJ, Whitney MS, Wolf AM, Scruggs DW. Heinz body hemolytic anemia associated with high plasma zinc concentration in a dog. *J Am Vet Med Assoc*. 1990;197:1347-1350.
6. Maxie MG, Newman SJ. Urinary system. In: Maxie MG, ed. *Jubb, Kennedy and Palmer's Pathology of Domestic Animals*. Edinburgh, UK: Elsevier; 2007:425-522.
7. Meurs KM, Breitschwerdt EB, Baty CJ, Young MA. Postsurgical mortality secondary to zinc toxicity in dogs. *Vet Hum Toxicol*. 1991;33:579-583.
8. Mikszewski JS, Saunders HM, Hess RS. Zinc-associated acute pancreatitis in a dog. *J Small Anim Pract*. 2003;44:177-180.
9. Onosaka S, Tetsuchikawahara N, Min KS. Paradigm shift in zinc: metal pathology. *Tohoku J Exp Med*. 2002;196:1-7.
10. Tetsuchikawahara N, Min KS, Onosaka S. Attenuation of zinc-induced acute pancreatitis by zinc pretreatment: Dependence on induction of metallothionein synthesis. *Journal of Health Science*. 2005;51:379-384.
11. Weingart C, Kohn B. Zinc intoxication in a Yorkshire Terrier due to Euro cent ingestion. *Schweiz Arch Tierheilkd*. 2009;151:75-81.
12. Newman SJ. The urinary system. In: Zachary JF, McGavin MD, eds. *Pathologic Basis of Veterinary Disease*. 5th ed. St. Louis, MO: Elsevier; 2012:600-602, 632.
13. Brockus CW. Erythrocytes. In: Latimer KS, ed. *Duncan & Prasse's Veterinary Laboratory Medicine Clinical Pathology*. 5th ed. Ames, Iowa: Wiley-Blackwell; 2011:12-13.
14. Tripathi NK, Gregory CR, Latimer KS. Urinary system. In: Latimer KS, ed. *Duncan & Prasse's Veterinary Laboratory Medicine Clinical Pathology*. 5th ed. Ames, Iowa: Wiley-Blackwell; 2011:262.